Inorganic Chemistry

Article

pubs.acs.org/IC

Drastic Differences between the Local and the Average Structures of $Sr_2MSbO_{5.5}$ (M = Ca, Sr, Ba) Oxygen-Deficient Double Perovskites

Graham King,* Kyle J. Thomas, and Anna Llobet

Lujan Neutron Scattering Center, Los Alamos National Laboratory, Los Alamos, New Mexico 87545, United States

Supporting Information

ABSTRACT: For many disordered materials, knowing their average crystal structure is insufficient for explaining and predicting their macroscopic properties. It has been found that a description of the short-range atomic arrangements is needed to understand such materials. In order to understand the conduction pathways in ionic conductors which have random distributions of vacancies it is imperative to know the local structures which are present. In this study the local structures of three oxygen-deficient double perovskites, $Sr_2MSbO_{5.5}$ (M = Ca, Sr, Ba), have been investigated by neutron pair distribution function analysis. The ions in these compounds are all found to have local coordination environments which are radically different than those given by their average structures. While there is no long-range ordering of the oxygen vacancies in these compounds, a considerable amount of short-range order does exist. The conditions which drive the short-range ordering are discussed as are the possible mechanisms for achieving it. It is proposed that the SbO_5 polyhedra form distorted trigonal bipyramids by moving oxygen atoms into interstitial positions. In the M = Sr compound 45° rotations of SbO_6 octahedra are also present, which add additional oxygen atoms into the interstitial sites. Large displacements of the Ca^{2+}, Sr^{2+}, and Ba^{2+} cations are also present, the directions of which are correlated with the occupancies of the interstitial oxygen sites. Reverse Monte Carlo modeling of the pair distribution function data has provided the actual bond length distributions for the cations.

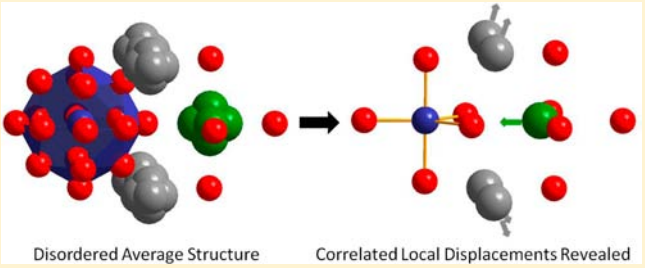

1. INTRODUCTION

The high ionic conductivities exhibited by many oxygen-deficient perovskites make them promising materials for a wide variety of applications, such as anode materials in solid oxide fuel cells.[1,2] In order to understand and improve the performance of such materials a proper knowledge of the arrangement of the atoms within the material is needed. It is well established that for many functional materials the local arrangements of atoms can differ significantly from the long-range average structures given by standard crystallographic methods. When this is the case, the local structure is usually more successful at explaining the observed properties. The key to understanding ionic conductivity is identifying what sites the mobile ions sit on as well as the activation energies required for moving between these sites. The actual local coordination environments of the atoms are much more important for understanding the conduction pathways than is knowledge of the average atomic positions.[3]

This study concerns the local structures of three compounds which have double-perovskite crystal structures. The double-perovskite structure, $A_2BB'O_6$, consists of a corner-sharing network of BO_6 and $B'O_6$ octahedra, where each BO_6 octahedron is connected at all six corners to a $B'O_6$ octahedron, and vice versa. The *A*-site cations occupy the large voids that exist between 4 BO_6 and 4 $B'O_6$ octahedra. The structure is shown in Figure 1. The three compounds which are the subject of this study have compositions of $Sr_2MSbO_{5.5}$, where M refers only to composition and not to a specific site and can be Ca, Sr, or Ba. There are

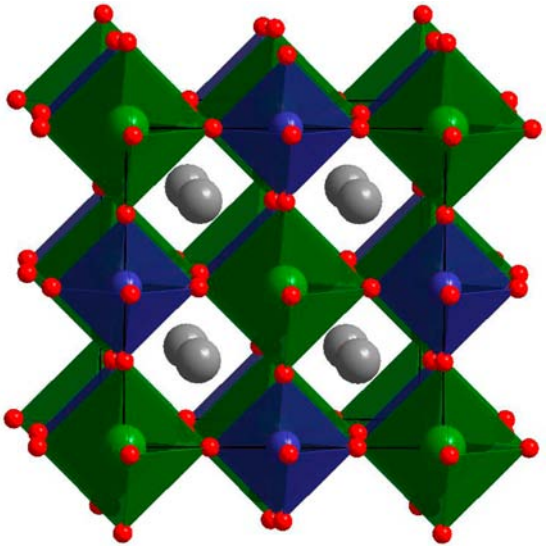

Figure 1. Double perovskite structure. Small blue spheres are *B*′-site cations, large green spheres are *B*-site cations, large gray spheres are *A*-site cations, and small red spheres are oxygen anions. Atomic coordinates used to generate this figure are those of the average structure of $Sr_3SbO_{5.5}$.

Received: October 19, 2012
Published: November 14, 2012

dx.doi.org/10.1021/ic302310y | *Inorg. Chem.* 2012, 51, 13060−13068

two distinctive features which are common to all three compositions. One is that they all have 1/12 of the anion sites vacant, giving formulas of $A_2BB'O_{5.5}$. The second is they all have unusually large cations occupying the *B*-sites (either Ca^{2+} or Sr^{2+}) and the small Sb^{5+} cation on the *B*′-site.

The average crystal structures and conductivities of several $A_2BB'O_{5.5}$ compounds which have very large *B*-site cations have been reported previously.[4−9] These compounds all have ideal cubic double-perovskite average structures with space group *Fm*-3*m* and no long-range ordering of the oxygen vacancies. They also share a tendency to absorb water to form hydrated compounds. The three $Sr_2MSbO_{5.5}$ (M = Ca, Sr, Ba) compounds which are the subject of this study have been recently reported to display anomalous thermal expansion behavior which is postulated to be caused by changes in clustering of water molecules and anion vacancies upon heating.[4] Another study has found that the $Sr_3SbO_{5.5}$ compound displays oxide ion conductivity at intermediate temperatures.[5] The average structure and conductivity properties of the related compound $SrCa_2SbO_{5.5}$ have been reported recently as well.[6] There are also compounds in which Sb^{5+} has been replaced by Nb^{5+} or Ta^{5+}, such as $Sr_3NbO_{5.5}$ and $Sr_3TaO_{5.5}$.[7−9] These compounds have been observed to conduct protons under wet conditions.[7] Some oxygen stoichiometric compounds with 1:2 *B*/*B*′ ratios are also known, such as $Sr_4Nb_2O_9$ ($SrSr_{1/3}Nb_{2/3}O_3$), which appear to share some structural similarities with the $A_2BB'O_{5.5}$ compounds.[10]

Numerous results reported in previous studies suggest that the local structures of these materials are quite different from their average structures. Despite this, no detailed analysis of the local structures has been carried out. Features observed in high-resolution transmission electron microscopy images of $Sr_3SbO_{5.5}$ have suggested that short-range ordering of oxygen vacancies may be present, but no details on the nature of this order were given.[5] Also, several papers have noted that the powder diffraction patterns of these materials have anomalous modulated backgrounds due to large amounts of diffuse scattering.[4,8,10] The modulations are much larger in the neutron powder diffraction patterns compared to the X-ray powder diffraction patterns, suggesting that there is a large amount of disorder in the oxygen atom positions. Another interesting finding is that some of the oxygen atoms appear to lie in interstitial positions quite far away from the double-perovskite anion site.[4,8] Similar disorder of the oxygen atoms has been observed in the highly disordered double-perovskite $Ba_{11}W_4O_{23}$.[11] The most recent structural refinements performed on the three $Sr_2MSbO_{5.5}$ (M = Ca, Sr, Ba) compounds used split positions for most of the atoms to account for the highly disordered structures.[4] These refinements give very large atomic displacement parameters for most atoms as well as unrealistic bond distances. While such models do provide an approximate description of the average structures, they do not provide any insight into the short-range correlations between local displacements that must be present.

In this work neutron pair distribution function (PDF) analysis is used to provide a detailed description of the local structures of the three $Sr_2MSbO_{5.5}$ (M = Ca, Sr, Ba) compounds. The PDF gives the radial distribution of interatomic distances in a material. A PDF is obtained by taking the sine Fourier transform of a total scattering pattern, which includes both Bragg and diffuse scattering. By analyzing the scattering at all values of *Q* this method makes explicit use of the information about the local structure which is contained in the diffuse scattering. PDF analysis has been successfully used in the past to provide important local structure information on other simple perovskites with high ionic conductivities.[12,13] For the $Sr_2MSbO_{5.5}$ (M = Ca, Sr, Ba) double perovskites the PDF analysis shows that the local structures of these materials are completely different from their average structures.

2. EXPERIMENTAL SECTION

The starting materials used for the synthesis were Sb_2O_3 (Fisher Scientific, 99.7%), $CaCO_3$ (Fisher Scientific, 99.8%), $SrCO_3$ (Alfa Aesar, 99.99%), and $BaCO_3$ (Fisher Scientific, 99.8%). Powders of the starting materials were mixed in stoichiometric ratios and ground together with a mortar and pestle. A 15% excess of Sb_2O_3 was needed to account for the high-temperature evaporation of this substance. Mixtures were heated in alumina crucibles at 1000 °C for 12 h. Samples were then reground and heated to 1200 °C for 36 h.

Initial characterization of the samples was done using a Bruker D8 X-ray powder diffractometer. Neutron total scattering data was collected at 300 K on the HIPD instrument at the Lujan Neutron Scattering Center at Los Alamos National Laboratory. In order to ensure that the samples did not contain any absorbed water they were heated to 325 °C for several hours and then immediately transferred to a He-filled glovebox where they were sealed in vanadium cans. Rietveld refinements were performed using the GSAS/EXPGUI software package.[14,15] The pair distribution functions were obtained by reducing the total scattering data using the PDFgetN program using a Q_{max} of 32 $Å^{-1}$.[16] These PDFs were fit using the PDFgui and RMCProfile programs.[17,18] For this work we use the following definition of the pair distribution function: $G(r) = 4\pi r[\rho(r) - \rho_0]$, where $\rho(r)$ is the microscopic pair density, ρ_0 is the average pair density, and *r* is the radial distance in Angstroms.

3. RESULTS AND DISCUSSION

3.1. Determination of the Average Structures. The X-ray and neutron powder diffraction patterns of all three compounds could be indexed using the cubic space group *Fm*-3*m*. No additional impurity peaks were observed, indicating that all samples were phase pure. The backgrounds of both the X-ray and the neutron powder diffraction patterns clearly showed anomalous modulations that were not accounted for by the instrumental backgrounds. The modulations in the neutron diffraction patterns were much more pronounced than the modulations in the X-ray diffraction patterns, indicating that the oxygen atom positions contain the greatest amount of disorder. The relative intensities of the modulations in the backgrounds of the neutron powder diffraction patterns increase in the following order based on the M cation: Ca < Ba < Sr.

A starting point for understanding the local structures of these materials is determining the long-range average crystal structures. In order to solve the crystal structures Rietveld refinements were performed on the neutron powder diffraction patterns using double-perovskite models. In double perovskites the smaller cations will preferentially occupy the *B* and *B*′-sites. In $Sr_2CaSbO_{5.5}$, the Sr cations occupy the *A*-site while Ca and Sb occupy the *B* and *B*′ positions. In $Sr_3SbO_{5.5}$, strontium occupies both the *A* and the *B* positions (hereafter referred to as Sr_A and Sr_B) while Sb occupies the *B*′ position ($Sr_2SrSbO_{5.5}$). In $Sr_2BaSbO_{5.5}$, the Ba cations occupy half of the *A*-sites while Sr occupies the other half. Sr also occupies the *B* position, while Sb again occupies the *B*′ position. In standard $A_2BB'O_{5.5}$ perovskite notation this would be written as $(Sr_{0.5}Ba_{0.5})_2SrSbO_{5.5}$. These assignments were previously confirmed using synchrotron powder diffraction.[4]

The Rietveld refinements produced results which matched closely with previously reported results and therefore will not be discussed in detail. Initial refinements were done using a simple cubic double-perovskite model. The structural parameters and bond distances obtained from these refinements are listed in Tables S1 and S2 of the Supporting Information. These refinements

dx.doi.org/10.1021/ic302310y | Inorg. Chem. 2012, 51, 13060−13068

were not able to produce fully satisfactory fits. Since previous studies have found that some of the oxygen atoms reside in interstitial sites new refinements were performed where a second O site at Wyckoff position 48*h* was added and the occupancies of the two oxygen sites were allowed to refine. This significantly improved the fits, especially in the case of $Sr_3SbO_{5.5}$. The final refined lattice parameters, oxygen site occupancies, and bond lengths obtained from these refinements are listed in Table 1.

Table 1. Lattice Parameters (*a*), Bond Lengths, and Occupancies (occ) of the Perovskite Anion Sites (O(1), 24*e* site) and Interstitial Sites (O(2), 48*h* site) as Determined from Rietveld Refinements of the Neutron Powder Diffraction Patterns

	$Sr_2CaSbO_{5.5}$	$Sr_3SbO_{5.5}$	$Sr_2BaSbO_{5.5}$
a (Å)	8.2303(2)	8.3203(5)	8.4512(4)
Sb−O(1) (Å)	1.995(2)	2.074(3)	1.966(1)
Sb−O(2) (Å)	3.112(5)	1.893(2)	3.161(3)
B−O(1) (Å)	2.119(2)	2.086(3)	2.259(1)
B−O(2) (Å)	1.802(4)	3.123(2)	1.955(2)
A−O(1) (Å)	2.910(1)	2.942(2)	2.991(1)
A−O(2) (Å)	2.336(5)	2.330(1)	2.351(3)
occ O(1)	0.744(2)	0.608(2)	0.728(2)
occ O(2)	0.083(1)	0.150(1)	0.095(1)

A complete list of structural parameters is given in Table S3 of the Supporting Information. The occupancies of the interstitial sites are correlated directly with the intensities of the background modulations in the diffraction patterns. Slight differences in the structural parameters in Table 1 compared to those given in ref 4 could be due to the fact that the compounds studied in ref 4 were hydrated while the ones used in this study were not. One important result of the refinements worth mentioning is that extremely large atomic displacement parameters were obtained for all atoms except the Sb atoms. This can be taken as an indication that in each of these compounds all atoms except Sb are locally displaced from their average positions.

3.2. Inadequacy of the Average Structure Descriptions. Inspection of the bond lengths in Table 1 indicates that there are some very serious problems with the average structures of these compounds. Many of these bond lengths are physically unrealistic. In addition, these bond lengths do not correspond to the features observed in the experimental PDFs. In order to see how the local structures differ from the average structures the experimental PDFs were compared with PDFs calculated from the average structure models obtained from the Rietveld refinements, as shown in Figure 2. As is immediately apparent, the calculated PDFs completely fail to reproduce the features observed in the experimental PDFs. One of the largest problems with the calculated PDFs is that they all have large peaks at ∼1.6 Å due to O(1)−O(2) distances. These peaks are completely absent in the experimental PDFs. The experimental PDFs were also compared with PDFs calculated from simple double-perovskite models without O in interstitial sites since such models do not have these short O−O distances. While these fits do not produce peaks at ∼1.6 Å, they fit even worse elsewhere and overall the fits are also very poor (see Figure S1 in the Supporting Information).

Some preliminary information regarding the local structures can be gained by assigning the features in the experimental PDFs to specific interatomic distances. The first sharp peak in each of the experimental PDFs can be assigned to Sb−O bond distances. This peak has its maximum at the exact same value for all three

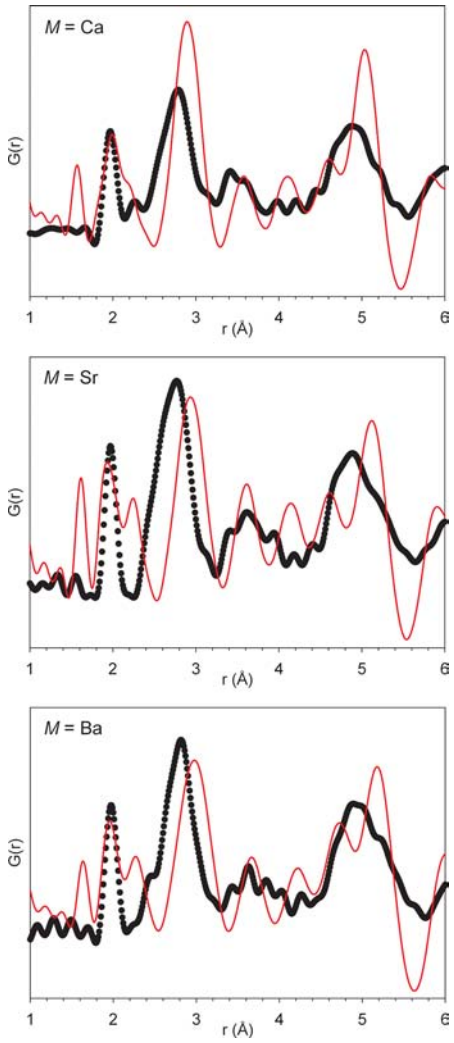

Figure 2. Calculated PDFs using the average structure as models (red lines) and experimental PDFs (black dots) for the three $Sr_2MSbO_{5.5}$ compounds.

compounds, 1.97 Å. This shows that the local coordination environments around the Sb^{5+} cations are largely unaffected by the overall composition of the compound. A value of 1.97 Å is exactly what would be expected from a mixture of 5- and 6-coordinate Sb^{5+} since, according to bond valence sum calculations, the average Sb−O bond lengths should be 1.94 and 2.01 Å, respectively. The average structures all show that Sb makes a bond to either the O(1) or the O(2) of about this length but also another bond to the other type of O of a much different length. These much longer Sb−O bond lengths are almost certainly not actually present. The strong highly covalent Sb−O bonds can be expected to create SbO_6 and SbO_5 molecular-like units with narrow bond length distributions. The sharpness of the first peak of the experimental PDFs confirms this expectation.

The third large peaks in the calculated PDFs between 2.0 and 2.3 Å are due to the *B*−O(1) bond lengths. However, these peaks are completely absent from the experimental PDFs, showing that there are essentially no such bond lengths in these compounds. This is not surprising since bonds of such length would be much shorter than expected for these cations. Indeed, bond valence sum calculations based on the bond lengths in the average structures reveal a severe overbonding of all the *B*-site cations for all compounds. The *B*−O(2) bond lengths are also far too short for

dx.doi.org/10.1021/ic302310y | *Inorg. Chem.* 2012, 51, 13060−13068

the M = Ca and Ba compounds, and the PDFs show that these bond lengths are not present either. The fourth large peaks in the calculated PDFs between 2.9 and 3.0 Å are due to A−O(1) bond lengths. The experimental PDFs show that the average A−O bond is actually slightly shorter than this. The A−O(2) bond lengths are unrealistically short, and it is unlikely that there are such short A−O bonds in any of these compounds. The experimental PDFs have just one broad peak which encompasses all the B−O, A−O, and O−O distances.

In order to fit the PDFs the large-box reverse Monte Carlo (RMC) method was employed. The method uses large supercells and adjusts the atomic positions to produce configurations which have interatomic distance distributions which fit the experimental PDFs. Since any description of the local structure cannot involve fractional occupancies of atoms the starting models used to generate the supercells were the simple double-perovskite structures obtained from the Reitveld refinements that did not allow oxygen in interstitial positions. These models were expanded into 8 × 8 × 8 supercells each containing 19 456 atoms. The vacancies and oxygen atoms were randomly swapped to produce a random distribution of vacancies before the atomic positions were allowed to refine. The O and vacancy sites were also allowed to swap during the refinements. Surprisingly, these refinements did not converge to produce good fits to the data. The final fits were quite poor and contained unrealistic bond length distributions. The refinements did not manage to move any of the oxygen atoms into interstitial sites. Additional refinements were attempted where the oxygen atoms were allowed to randomly swap with vacant interstitial positions. These refinements also did not converge to produce good fits or find chemically reasonable placements for interstitial O atoms. It appears that the average structures differ so greatly from the true local structures that the RMC refinements are unable to convert from one to the other. This in itself is a remarkable result.

3.3. Conditions Requiring Local Order. In order to solve the local structures it was necessary to devise starting models for the RMC refinements which more closely resembled the true local structures than the double-perovskite models did. This was done by considering possible mechanisms to relieve the bond strains that are present in the average structures. The major problems with the average structures are that the B−O bond lengths are far too short while the A−O bond lengths are slightly too long. In addition, the coordination numbers (CNs) of the B-site cations are too small, being 5 one-half the time and 6 one-half the time. While a CN of 5 is perfectly acceptable for a small cation like Sb^{5+}, it is unreasonably small for large cations like Ca^{2+} and Sr^{2+}. These cations will prefer CNs of at least 6.

The Rietveld refinements show that some of the oxygen atoms reside in interstitial positions. It is worthwhile to briefly consider the consequences of putting oxygen atoms into these interstitial positions. In the ideal double-perovskite structure each O atom is coordinated by one B cation, one B' cation, and four A cations. By moving into an interstitial position, the O is now coordinated to one B' cation, two B cations, and three A cations. This translates into a reduction in the A-site CN and an increase in the B-site CN, exactly what is needed to stabilize the structure. However, the new bond distances that form are unfavorable. The two B−O bonds are now extremely long, and one of the three A−O bonds is very short. Therefore, moving O into interstitial positions improves the situation in terms of the coordination numbers but does not by itself lead to a stable structure.

While previous studies have described the O atoms as being statistically distributed among the double-perovskite anion sites and the interstitial sites, this obviously cannot be the case as it would result in unrealistically short O−O distances. In order for an oxygen atom to occupy an interstitial site while avoiding short O−O contacts two conditions must be fulfilled.

(1) Both of the neighboring double-perovskite anion sites must be vacant as these are only about 1.62 Å away from the interstitial site.

(2) The 5 closest other interstitial sites must also be vacant as these are only about 1.96 Å away.

Besides O−O distances of 1.62 or 1.96 Å being energetically unrealistic, the PDFs clearly show that no such distances exist (Figure 2). One important consequence of condition 2 which is worth noting is that it immediately implies that no more than 1/6 of all the interstitial sites can be occupied. The M = Sr compound is actually near this limit, while the other two compounds are well below this limit. The two conditions listed above are highly restrictive and require a large degree of local order to ensure an energetically reasonable structure. As will be discussed later, there is also an additional consideration which further restricts which interstitial sites can be occupied.

There are only two possible mechanisms for allowing oxygen atoms to occupy interstitial positions while not violating condition 1. One mechanism is for some of the SbO_6 and/or SbO_5 to rotate by ∼45° about one of the double-perovskite cell axes. As shown in Figure 3, a 45° rotation of an SbO_6 octahedron

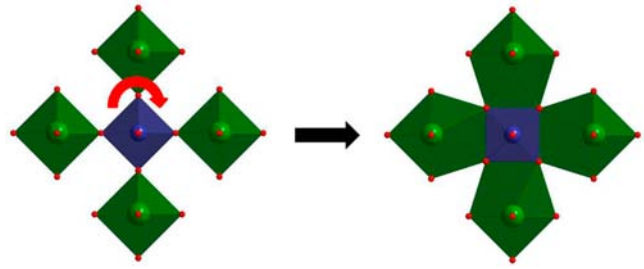

Figure 3. Movement of oxygen atoms into interstitial sites by 45° rotations of SbO_6 octahedra (blue). Green polyhedra are BO_6 or BO_7 units.

will move 4 of the 6 oxygen atoms into interstitial positions while simultaneously vacating all four of the neighboring perovskite anion sites. Such 45° rotations of smaller $B'O_6$ octahedra are known to occur in several anion stoichiometric double-perovskite compounds which also have very large size differences between the B and the B' cations and small tolerance factors.[19−27] One such compound is the closely related Sr_3WO_6.[19] In such compounds the 45° rotations serve to increase the coordination numbers of the larger B-site cations. As can be seen in Figure 3, the larger B-site cations (green) increase their coordination number to 7 by sharing an edge with the small B' cation (blue).

The other mechanism for moving oxygen into interstitial sites is for the SbO_5 square pyramids which are formed by the oxygen vacancies to transform into distorted trigonal bipyramids. This is illustrated in Figure 4. If all the SbO_5 polyhedra were to be trigonal bipyramids this would result in 2/11 of the O atoms residing in interstitial positions.

Both of these mechanisms can lead to more stable structures by having large displacements of the B-site cations which are correlated with the locations of the interstitial oxygen atoms.

dx.doi.org/10.1021/ic302310y | Inorg. Chem. 2012, 51, 13060−13068

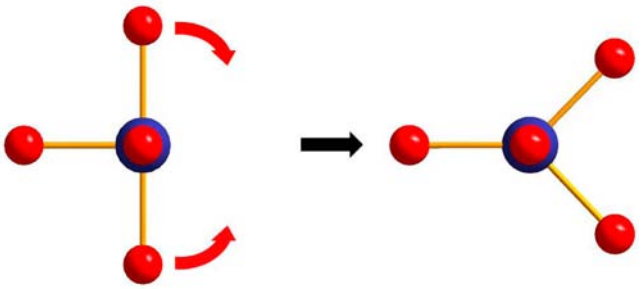

Figure 4. Formation of SbO_5 distorted trigonal bipyramids by movement of oxygen into interstitial positions around an oxygen vacancy.

This is shown in Figures 5 and 6. Figure 5a shows the coordination environment of a *B*-site cation which results from

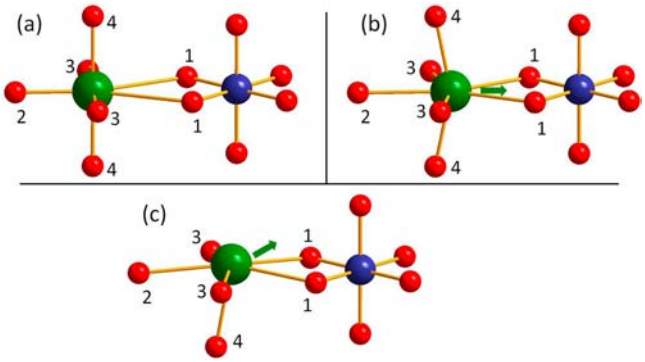

Figure 5. *B*-site coordination environments created by 45° rotations of SbO_6 octahedra. Rotation of one-half of the SbO_6 octahedra will lead to 50% of the *B*-site cations having the coordination shown in b and 50% having the coordination environment shown in c.

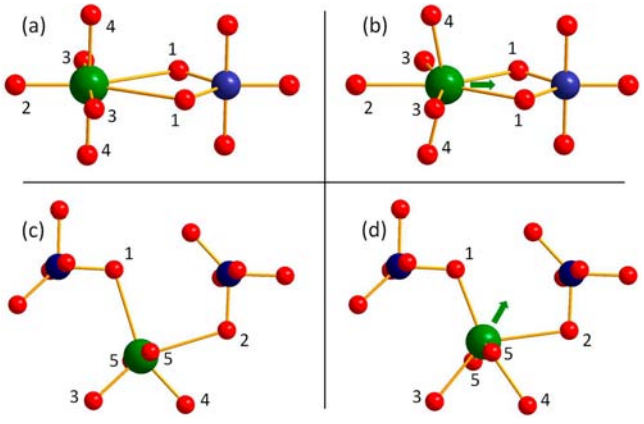

Figure 6. *B*-site coordination environments created by formation of SbO_5 trigonal bipyramids. If all SbO_5 polyhedra form trigonal bipyramids then one-half of the *B* cations will have the coordination environment shown in b and one-half will have the coordination environment shown in d.

having one neighboring SbO_6 octahedron which has been rotated by 45°. The 45° rotation results in the corner sharing between these two polyhedra being replaced by edge sharing. The bonds from the *B*-site cation to the O of the shared edge (O1 in Figure 5) are very long (~3.1 Å). This allows the *B*-site cation to shift toward the oxygen atoms which are part of the shared edge as shown in Figure 5b. Even after a large shift the bonds to the O1 atoms will still remain long. In addition, the bond to the O2 atom will be significantly elongated while the remaining four short bonds are also elongated very slightly. This helps to greatly reduce the overbonding of the *B*-site cation. Formation of trigonal bipyramids also leads to edge sharing between SbO_5 polyhedra and *B*-site cations, as shown in Figure 6a. In this case the *B*-site cation will also displace toward the shared edge (Figure 6b) to produce a similar coordination environment for the *B*-site cation.

Depending on the fraction of SbO_6 and/or SbO_5 that are rotated by 45° a *B*-site cation may share more than one edge with surrounding Sb-centered polyhedra. As pointed out by Abakumov et al., it is unfavorable for a *B*-site cation to have two shared edges *trans* to each other as this frustrates the direction of the displacement of the *B*-site cation.[20] Therefore, shared edges will only occur in one of the four *cis* positions but not in the *trans* position. Formation of SbO_5 trigonal bipyramids also can lead to situations where a *B*-site cation makes a bond to just one of the two interstitial O atoms on a SbO_5 polyhedra. If this occurs more than once per *B*-site cation (Figure 6c and 6d) these O will also not occupy trans positions. These considerations can be summarized as a third general condition.

(3) Large displacements of *B*-site cations toward interstitial O atoms will help eliminate very short B−O bonds. An O atom will never occupy an interstitial site which is *trans* to another occupied interstitial site on a *B*-site cation coordination sphere as this would frustrate the direction of the *B*-site cation displacement.

3.4. Modeling and RMC Fitting. Several model structures were constructed to serve as starting points for RMC refinements. The modeling of the M = Ca and Ba compounds will be discussed together since both have similar concentrations of O in interstitial sites. The Rietveld refinements indicate that both compounds have about 2/11 of the O atoms in interstitial sites. This can be accomplished by having all of the SbO_5 form trigonal bipyramids or one-half of all the SbO_6 octahedra (1/4 of all the Sb centered polyhedra) rotated by 45°. A model was constructed for each of these two possibilities. The model structures were made by manually moving O atoms within a 2 × 2 × 2 double-perovskite supercell into interstitial positions by either rotating entire SbO_6 octahedra or transforming SbO_5 square pyramids into distorted trigonal bipyramids. The choices of which polyhedra were altered was not chosen randomly but done in such a way as to ensure that the three conditions outlined in section 3.3 were not violated.

The coordination environments generated for the *B*-site cations from this procedure are shown in Figures 5 and 6. Rotating one-half of all the SbO_6 octahedra results in all *B*-site cations sharing one edge with an SbO_6 octahedron. One-half of the *B*-site cations will have the coordination geometry shown in Figure 5b. The other half will have one vacancy around them, giving the coordination geometry shown in Figure 5c. The location of the vacancy is unlikely to be random. For example, it is unlikely to be at position 2. Since the O2 atom is already forming a long bond it would be an energetic waste to remove this oxygen. It would be much more favorable to remove one of the remaining 4 short bonds. While the difference between removing an O3 atom or an O4 atom is probably not large, removal of O4 seems slightly favored as the resulting *B*-site cation shift will still make equal bond lengths to the two O1 atoms. It was the O4 atoms that were removed in constructing the models. Removal of this atom also allows the *B*-site cation

dx.doi.org/10.1021/ic302310y | *Inorg. Chem.* 2012, 51, 13060−13068

to shift away from the other O4 atom, leaving only two short bonds (Figure 5c).

Having all the SbO_5 polyhedra form distorted trigonal bipyramids will give one-half of the *B*-site cations the coordination geometry shown in Figure 6b. Notice how this is essentially the same geometry as one-half the *B*-site cations have when one-half of all the SbO_6 octahedra are rotated. The other half of the *B*-site cations will have coordination geometry similar to what is shown in Figure 6c. These cations are coordinated by two interstitial oxygen atoms from two different SbO_5 polyhedra (atoms 1 and 2 in Figure 6c). Since these are very long bonds the *B*-site cation will shift toward them, significantly elongating the bonds to atoms 3 and 4 and very slightly elongating the bonds to the atoms labeled 5. This results in a configuration with 4 long and only 2 short bonds, which relieves the underbonding of the *B*-site cation.

These two models were expanded into 4 × 4 × 4 supercells (8 × 8 × 8 supercells of the double-perovskite structures) to be used for RMC fitting. The RMC fits using either model were able to provide excellent fits to the experimental PDFs for both the M = Ca and Ba compounds (Figure 7). While these two models

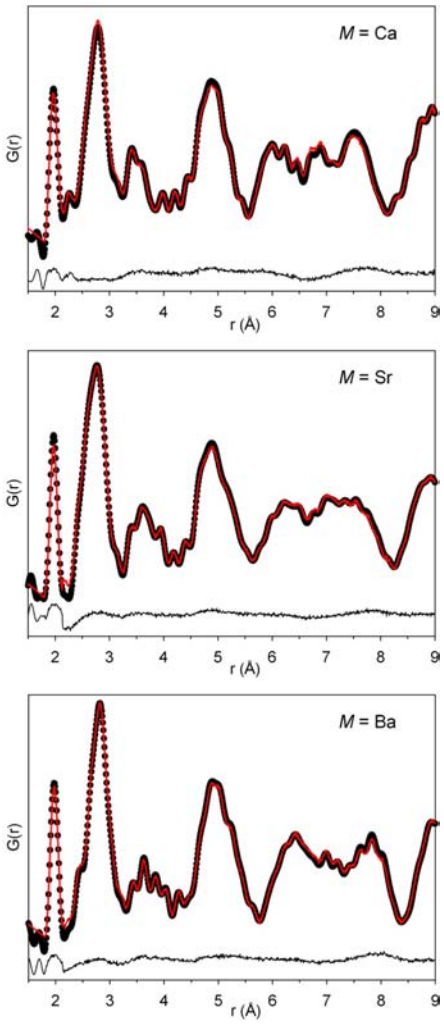

Figure 7. RMC fits (red lines) to the experimental PDFs (black dots) and the difference curves (beneath) for the three $Sr_2MSbO_{5.5}$ compounds.

are fundamentally different and the RMC algorithm is not able to interconvert between the two, the two models give very similar bond length distributions for all of the cations and therefore give very similar fits. The two models do produce slightly different nearest neighbor O−O distance distributions due to the different O−O distances inherent to square pyramidal SbO_5 units (in the 45° rotation model) and distorted trigonal bipyramidal SbO_5 units (in the trigonal bipryamidal model). However, this difference is not large enough to make a significant contribution to the overall intensity of the PDFs, and therefore, these two models cannot be reliably differentiated based on the RMC fits. Although it is not possible to tell which model is correct based on the fits, the two models give the exact same distributions of coordination numbers for all cations as well as very similar bond length distributions. Therefore, the results presented in section 3.5 can be considered to be accurate regardless of which model is correct.

There are several reasons to favor the model with SbO_5 trigonal bipyramids over the model with 45° rotations of the SbO_6. The first is that a distorted trigonal bipyramidal geometry can be expected to be energetically favorable since it reduces O−O repulsion. In an SbO_5 square pyramid (assuming an Sb−O distance of 1.94 Å) there will be 8 O−O distances at ∼2.74 Å. If distorted trigonal bipyramids are formed instead, such that the two oxygen atoms in the interstitial positions form ∼90° O−Sb−O angles, there will be only 7 O−O distances at ∼2.74 Å and two much longer ones at ∼3.58 Å. Second, in the few known examples of 5-coordinated Sb^{5+}, such as the SbF_5 molecule, trigonal bipyramidal geometry is observed. Third, the coordination environment shown in Figure 6d is more symmetric than the one shown in Figure 5c, making it seem more likely. Fourth, the concentration of O in interstitial sites (2/11) for these compounds is exactly the value expected if all SbO_5 formed trigonal bipyramids. If 45° rotations were occurring any value between 0 and 1/3 would be possible. This is probably not just a coincidence and serves as additional supporting evidence for the existence of SbO_5 trigonal bipyramids.

The $Sr_3SbO_{5.5}$ compound has a considerably higher concentration of O atoms in interstitial positions compared to the other two compounds (∼1/3 of all O). It is not possible to have this high a concentration of interstitial O atoms just by formation of SbO_5 trigonal bipyramids; therefore, some 45° rotations of Sb-centered polyhedra must be present. There are two ways to have 1/3 of all O atoms in interstitial positions. One is to have ∼45% of all the SbO_6 and/or SbO_5 polyhedra rotated by 45°. The other is to have all SbO_5 form trigonal bipyramids and ∼40% of the SbO_6 also rotate by 45°. Since these two models will produce essentially the same bond length distributions they cannot be differentiated by RMC fitting. Since, for the reasons discussed above, SbO_5 trigonal bipyramid formation seems likely the model used for the RMC fitting was one with both SbO_5 trigonal bipyramids and 45° rotation of SbO_6 octahedra in addition to that. This model was also constructed by manually moving atoms within a 2 × 2 × 2 supercell and assuring that this was done so not to violate the conditions outlined in section 3.3. RMC refinements using this model were able to provide a good fit to the data as shown in Figure 7.

3.5. Results of the RMC Fits. The atomic configurations obtained from the RMC analysis provide the distributions of interatomic distances for all atom−atom pairs. The distributions of Sb−O distances are essentially the same for all three compounds studied. All Sb−O distance distributions peak at 1.97 Å. The Sb−O distance distributions are quite narrow and indicate that the SbO_5 and SbO_6 polyhedra are highly regular.

According to the average crystal structures one-half of the *B*-site cations should have a CN of 5 and one-half should have a

dx.doi.org/10.1021/ic302310y | *Inorg. Chem.* 2012, 51, 13060−13068

CN of 6. While the average structure descriptions also give very short *B*−O bond distances in the range of 1.8− 2.3 Å, the PDFs show that there are actually extremely few *B*−O bonds at such short distances. The presence of O in interstitial sites coupled with large displacements of the *B*-site cations gives larger coordination numbers for the *B*-site cations as well as a very broad distribution of bond distances including many much longer *B*−O bonds. In $Sr_2CaSbO_{5.5}$ the number of O atoms in interstitial sites raises the CN of the Ca atoms by exactly 1, such that now one-half have a CN of 6 and one-half have a CN of 7. The *B*−O bond length distributions are shown in Figure 8 (all bond length distributions are given in the Supporting Information in Figure S2). The Ca−O distribution peaks at 2.26 and gives an average Ca−O bond length of 2.38 Å. In $Sr_2BaSbO_{5.5}$ the CNs of the Sr_B cations are about the same as in $Sr_2CaSbO_{5.5}$ although slightly higher on average due to the slightly higher concentration of O in interstitial positions. The average CN for the Sr_B cations is 6.6. The Sr_B−O distribution peaks at 2.42 Å and gives an average Sr_B−O bond length of 2.53 Å. In $Sr_3SbO_{5.5}$ the higher concentration of O atoms in interstitial positions results in the Sr_B cations having even higher CNs of 7 or 8, with an average CN of 7.3. The higher average CN also results in longer average bond lengths for the Sr_B cations than in $Sr_2BaSbO_{5.5}$. The Sr_B−O distribution peaks at 2.54 Å and gives an average Sr_B−O bond length of 2.59 Å. The displacements of the *B*-site cations (illustrated in Figures 5 and 6) needed to achieve the bond length distributions mentioned above are very large. Analysis of the RMC configurations reveals that the Ca or Sr_B cations are displaced by ∼0.45 Å relative to their positions in the double-perovskite average structures.

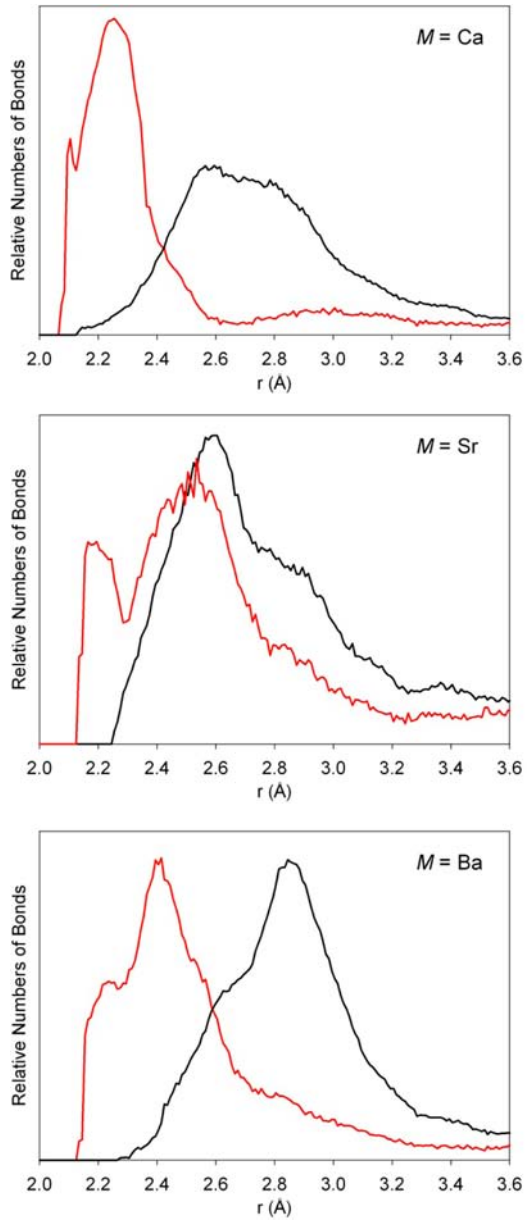

Figure 8. *B*−O (red) and *A*−O (black) bond length distributions obtained from the RMC fitting for the $Sr_2MSbO_{5.5}$ compounds.

The coordination environments of the *A*-site cations are also significantly altered by the presence of O atoms in interstitial sites. A coordination environment for an *A*-site cation that would be typical in the M = Ca or Ba compounds is shown in Figure 9.

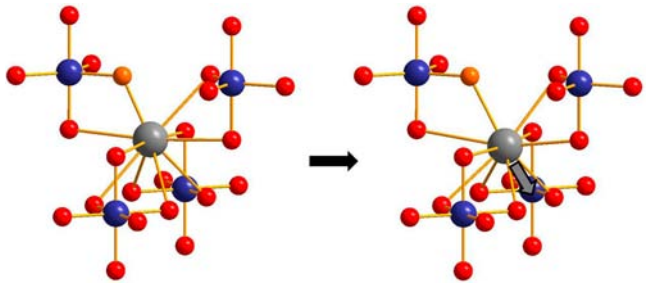

Figure 9. Typical *A*-site cation coordination environment in the M = Ca or Ba compounds. (Left) *A*-site coordination created by putting some oxygen atoms in interstitial sites. Orange atom is making a very short bond, while the other *A*−O bonds are long. (Right) How the *A*-site cation displaces to form a stable bonding environment.

In these compounds the average *A*-site cation will have a CN of about 10 (exactly 10 for the M = Ca compound and 9.9 for the M = Ba compound). Nine of these bonds will be long bonds (∼2.95 Å), and one bond, which is to an interstitial O (orange atom in Figure 9), will be very short (∼2.3 Å). The *A*-site cations will displace away from this short bond, elongating the bond. This displacement also serves to significantly shorten three of the long *A*−O bonds. Five or the remaining *A*−O bonds will change their distance only slightly, while one bond actually elongates to ∼3.2 Å and is now only semicoordinated. The overall *A*−O bond length distribution then consists of 4 short, 5 medium, and 1 long bond. The *A*−O bond length distributions are shown in Figure 8. The Sr−O distribution in $Sr_2CaSbO_{5.5}$ peaks at 2.56 Å and gives an average Sr−O bond distance of 2.77 Å. The *A*−O distribution in $Sr_2BaSbO_{5.5}$ peaks at 2.85 Å and gives an average *A*−O bond distance of 2.92 Å. While the RMC refinements cannot reliably separate out the Sr_A−O and Ba−O distributions, it is quite likely that the Ba−O bond lengths are considerably longer than the Sr_A−O bond lengths. In $Sr_3SbO_{5.5}$ the higher concentration of O in interstitial sites results in a lower average coordination number for the Sr_A cations of 9.2 and consequently more short Sr_A−O bonds. The distribution of Sr_A−O bond lengths peaks at 2.60 Å and has a distinct high *r* shoulder around 2.9 Å and a fair number of bonds at even higher distances. The average Sr_A−O bond length is 2.83 Å. An analysis of the configurations of atoms reveals that in all three compounds the *A*-site cations are displaced about 0.35 Å from their position in the double-perovskite structure.

dx.doi.org/10.1021/ic302310y | *Inorg. Chem.* 2012, 51, 13060−13068

3.6. Discussion and Comparison with Related Compounds. PDF analysis has shown that $Sr_2CaSbO_{5.5}$ and $Sr_2BaSbO_{5.5}$ have similar local structures, while the local structure of $Sr_3SbO_{5.5}$ is related but distinctly different. The reason for $Sr_3SbO_{5.5}$ being different can be traced to the tolerance factors of these compositions. The tolerance factor (τ) of a perovskite is a measure of how well the *A*-site cation fits within the structure. A τ of 1 indicates a perfect fit, while a τ of less than 1 indicates that the *A*-site cation is too small. In $Sr_2CaSbO_{5.5}$ the *B*-site cation (Ca) is smaller than the *A*-site cation (Sr), as is typical in perovskites. Since Ca is still a rather large *B*-site cation the tolerance factor is still small at 0.893. In $Sr_2BaSbO_{5.5}$, one-half of the *A*-site cations are larger than the *B*-site cation while the other half are the same size. Since Sr is a very large *B*-site cation a small tolerance factor of 0.903 results. In $Sr_3SbO_{5.5}$ the *A*- and *B*-site cations are the same size, leading to a highly strained structure with an even lower τ of only 0.877. The very high strain caused by putting Sr on both of the very differently sized *A* and *B*-sites can be considered the origin of the different local structure of $Sr_3SbO_{5.5}$.

It is informative to compare the $Sr_2MSbO_{5.5}$ compounds with their oxygen stoichiometric tungsten analogs, Sr_2MWO_6, since W^{6+} and Sb^{5+} have similar ionic radii. The double-perovskite Sr_2CaWO_6 crystallizes in space group $P2_1/n$ as a result of octahedral tilting about all three perovskite unit cell axes.[28,29] Tilting of the BO_6 and $B'O_6$ octahedra by not more than about 15° is very common in perovskites with tolerance factors below 1 and serves to reduce the coordination numbers of the *A*-site cations below 12 and shorten some of the remaining bonds. Since $Sr_2CaSbO_{5.5}$ and Sr_2CaWO_6 have essentially the same τ, it is worthwhile to consider why $Sr_2CaSbO_{5.5}$ does not display a common pattern of octahedral tilting. Having some of the oxygen atoms residing in interstitial positions ends up serving the same function as it also causes a reduction in the *A*-site CN and, through shifts of the *A*-site cations, produces several shorter *A*−O bonds. In addition, it also resolves a second instability by increasing the CN of the *B*-site cation. Standard octahedral tilting would not change the *B*-site CN and would leave one-half of the *B*-site cations with a CN of only 5, which is highly unfavorable for a larger *B*-site cations such as Ca. Furthermore, forming SbO_5 trigonal bipyramids is also favorable since it reduces O−O repulsion. While the crystal structure of Sr_2BaWO_6 has not been reported, it can be calculated to have a tolerance factor which is slightly larger than that of Sr_2CaWO_6. Since this is the case, it is reasonable to speculate that it would most likely adopt the $P2_1/n$ double-perovskite structure as well and the same arguments used to explain the local structure of Sr_2CaWO_6 would apply to it.

Unlike Sr_2CaWO_6, the crystal structure of Sr_3WO_6 does not involve a common pattern of octahedral tilting. Instead, in this structure 1/3 of the WO_6 octahedra are rotated by ∼45°, breaking the corner-sharing connectivity of the structure by replacing some of the corner sharing with edge sharing.[19] This unusual pattern of tilting is a result of the low tolerance factor and large mismatch in size between the Sr^{2+} and the W^{6+} cations. In $Sr_3SbO_{5.5}$ the likely formation of SbO_5 trigonal bipyramids puts 2/11 of the oxygen atoms into interstitial positions and helps relieve the bond strains. However, just as how in Sr_3WO_6 normal octahedral tiling patterns are insufficient to stabilize the structure, in $Sr_3SbO_{5.5}$ 2/11 of the oxygen in interstitial positions is not by itself sufficient to relieve the huge bond strains which are present. To further stabilize the structure additional O is added to the interstitial sites by the same type of ∼45° rotations that occur in Sr_3WO_6. About 40% of the SbO_6 octahedra are rotated by 45°, putting almost 1/3 of oxygen atoms into interstitial sites. The result is that the Sr on the *A* and *B*-sites now differ only slightly in CN and average bond length. While in the average structure the Sr_A and Sr_B cations differ in coordination number by 6 and in average bond length by 0.85 Å, in reality they only differ in CN by about 2 and in average bond length by about 0.24 Å. An interesting similarity between the two compounds is that in Sr_3WO_6 2/3 of the Sr_B cation have a CN of 7 and 1/3 have a CN of 8 and in $Sr_3SbO_{5.5}$ the CNs of the Sr_B cations are almost exactly the same (average CN 7.3). A higher fraction of O in interstitial sites is needed in $Sr_3SbO_{5.5}$ compared to Sr_3WO_6 to counter out the reduction in CN caused by oxygen vacancies. It is worth noting that in $Sr_2BaSbO_{5.5}$ there are some indications that a small (∼7%) fraction of the SbO_6 octahedra are rotated by 45°. The fraction of O in interstitial sites for this compound is slightly above the limit that can be caused by formation of SbO_5 trigonal bipyramids alone. It could be that if there are some local clusters of Sr_A cations (a local deficiency of Ba) then an SbO_6 octahedron in that cluster could tilt by 45° to accommodate the strain since locally the structure would resemble $Sr_3SbO_{5.5}$.

4. CONCLUSIONS

Reverse Monte Carlo modeling of neutron pair distribution function data for three $Sr_2MSbO_{5.5}$ (M = Ca, Sr, Ba) oxygen-deficient double perovskites has revealed that the local structures of these compounds are extremely different from their long-range average structures. It is proposed that in $Sr_2CaSbO_{5.5}$ and $Sr_2BaSbO_{5.5}$ the SbO_5 polyhedra form distorted trigonal bipyramids by having two of the oxygen atoms move into interstitial sites. This increases the coordination numbers of the *B*-site cations from values of 5 and 6 to values of 6 and 7 and decreases the coordination number of the *A*-site cations from 11 to 10. The movement of the oxygen into the interstitial sites is coupled with large displacements of the *A*- and *B*-site cations, giving broad bond length distributions which are totally different than the bond lengths given by the average structure descriptions. In $Sr_3SbO_{5.5}$ it is proposed that in addition to the SbO_5 polyhedra forming trigonal bipyramids some of the SbO_6 octahedra are also rotated by 45°. This puts additional oxygen atoms into interstitial sites, which is necessary to relieve the higher bond strains inherent to this composition. The result is that the Sr_B cations now have an average coordination number of 7.3 and the Sr_A cations have a coordination number of 9.2. These two cations now only have slightly different average bond lengths, as opposed to the much different bond lengths given by the average structure.

From these results it is apparent that any attempt to understand the ionic conduction pathways in these materials based on the average long-range structures would be hopeless. The conduction pathways depend on the local coordination environments of the cations, which have been determined in this study. It is likely that other oxygen-deficient double perovskites with very large size differences between the *B* and the *B'* cations such as $Sr_3NbO_{5.5}$ and $Sr_3TaO_{5.5}$ have similar local structures. A computational study based on the local coordination environments determined in this study would be helpful for elucidating the energetics of the oxide and proton conductivities for these compounds.

■ ASSOCIATED CONTENT

Supporting Information

Tables of crystallographic data, additional fits to the PDFs, and complete interatomic distance distributions from the RMC refinements. This material is available free of charge via the Internet at http://pubs.acs.org.

dx.doi.org/10.1021/ic302310y | *Inorg. Chem.* 2012, 51, 13060−13068

AUTHOR INFORMATION

Corresponding Author

*E-mail: gking@lanl.gov.

Notes

The authors declare no competing financial interest.

ACKNOWLEDGMENTS

This work has benefited from the use of HIPD at the Lujan Center at Los Alamos Neutron Science Center, funded by the DOE Office of Basic Energy Sciences. Los Alamos National Laboratory is operated by Los Alamos National Security LLC under DOE Contract No. DE-AC52 06NA25396. K.J.T. was funded by the Thurgood Marshall College Fund in partnership with the Department of Energy.

REFERENCES

(1) Norby, T. *J. Mater. Chem.* **2001**, *11*, 254−257.
(2) Fabbri, E.; Pergolesi, D.; Traversa, E. *Chem. Soc. Rev.* **2010**, *39*, 4355−4369.
(3) Stolen, S.; Bakken, E.; Mohn, C. E. *Phys. Chem. Chem. Phys.* **2006**, *8*, 429−447.
(4) Zhou, Q.; Kennedy, B. J.; Avdeev, M. *J. Solid State. Chem.* **2011**, *184*, 2559−2565.
(5) Chinarro, E.; Mather, G. C.; Caballero, A.; Saidi, M.; Moran, E. *Solid State Sci.* **2008**, *10*, 645−650.
(6) Moreno, B.; Urones-Garrote, E.; Chinarro, E.; Fuentes, L.; Moran, E. *Chem. Mater.* **2011**, *23*, 1779−1784.
(7) Jalarvo, N.; Haavik, C.; Kongshaug, C.; Norby, P.; Norby, T. *Solid State Ionics* **2009**, *180*, 1151−1156.
(8) Li, M.-R.; Hong, S.-T. *Chem. Mater.* **2008**, *20*, 2736−2741.
(9) Deniard, P.; Caldes, M. T.; Zou, X. D.; Diot, N.; Marchand, R.; Brec, R. *Int. J. Inorg. Mater.* **2001**, *3*, 1121−1123.
(10) Levin, I.; Chan, J. Y.; Scott, J. H.; Farber, L.; Vanderah, T. A.; Maslar, J. E. *J. Solid State Chem.* **2002**, *166*, 24−41.
(11) Hong, S. T. *J. Solid State Chem.* **2007**, *180*, 3039−3048.
(12) Malavasi, L.; Kim., H. J.; Proffen, T. *J. Appl. Phys.* **2009**, *105*, 123519.
(13) Norberg, S. T.; Hull, S.; Ahmed, I.; Eriksson, S. G.; Marrocchelli, D.; Madden, P. A.; Li, P.; Irvine, J. T. S. *Chem. Mater.* **2011**, *23*, 1356−1364.
(14) Larson, A. C.; Von Dreele, R. B. General Structure Analysis System (GSAS), Los Alamos National Laboratory Report LAUR 86-748, 2004.
(15) Toby, B. H. *J. Appl. Crystallogr.* **2001**, *34*, 210.
(16) Peterson, P. F.; Gutmann, M.; Proffen, Th.; Billinge, S. J. L. *J. Appl. Crystallogr.* **2000**, *33*, 1192.
(17) Farrow, C. L.; Juhas, P.; Liu, J. W.; Bryndin, D.; Bozin, E. S.; Bloch, J.; Proffen, Th.; Billinge, S. J. L. *J. Phys.: Condens. Matter* **2007**, *19*, 335219.
(18) Tucker, M. G.; Keen, D. A.; Dove, M. T.; Goodwin, A. L.; Hui, Q. *J. Phys.: Condens. Matter* **2007**, *19*, 335218.
(19) King, G.; Abakumov, A. M.; Hadermann, J.; Alekseeva, A. M.; Rozova, M. G.; Perkisas, T.; Woodward, P. M.; Van Tendeloo, G.; Antipov, E. V. *Inorg. Chem.* **2010**, *49*, 6058.
(20) Abakumov, A. M.; King, G.; Laurinavichute, V. K.; Rozova, M. G.; Woodward, P. M.; Antipov, E. V. *Inorg. Chem.* **2009**, *48*, 9336.
(21) King, G.; Abakumov, A. M.; Woodward, P. M.; Llobet, A.; Tsirlin, A. A.; Batuk, D.; Antipov, E. V. *Inorg Chem.* **2011**, *50*, 7792−7801.
(22) Stoger, B.; Weil, M.; Zobetz, E. *Z. Kristallogr.* **2010**, *225*, 125−138.
(23) Zuniga, F. J.; Tressaud, A.; Darriet, J. *J. Solid. State Chem.* **2006**, *179*, 3607.
(24) Withers, R. L.; Welberry, T. R.; Brink, F. J.; Noren, L. *J. Solid State Chem.* **2003**, *170*, 211.
(25) Bramnik, K. G.; Miehe, G.; Ehrenberg, H.; Fuess, H.; Abakumov, A. M.; Shpanchenko, R. V.; Pomjakushin, V. Yu.; Balagurov, A. M. *J. Solid State Chem.* **2000**, *149*, 49−55.
(26) Jeitschko, W.; Mons, H. A.; Rodewald, U. C.; Moller, M. H. *Z. Naturforsch.* **1998**, *53*, 31−36.
(27) Tomaszewska, A.; Muller-Buschbaum, H. *Z. Anorg. Allg. Chem.* **1993**, *619*, 1738−1742.
(28) Madariaga, G.; Faik, A.; Breczewski, T.; Igartua, J. M. *Acta Crystallogr.* **2010**, *B66*, 109−116.
(29) Gateshki, M.; Igartua, J. M. *J. Phys.: Condens. Matter* **2004**, *16*, 6639−6649.